

SCIENTIFIC
SECTION

Asymmetry of the parental craniofacial skeleton in orofacial clefting

G. T. McIntyre and P. A. Mossey

University of Dundee Dental School, UK

Abstract

Objective: To evaluate size-related and shape-related craniofacial skeletal asymmetries in the parents of children with orofacial clefting (OFC).

Design: Retrospective PA cephalometric study.

Setting: Glasgow/Dundee, Scotland.

Subjects: Ninety-two parental volunteers from a completely ascertained sample of 286 children born with OFC between 1980–1984 in the West of Scotland.

Interventions: None.

Main outcome measures: A conventional cephalometric asymmetry analysis (CCAA) evaluated size-related right:left asymmetry comprising eight linear distance, nine angular, and three mid-facial area measurements. The right and left landmark configurations were uniformly scaled using Procrustes superimposition and Euclidean Distance Matrix Analysis (EDMA) evaluated shape-related right-left asymmetry

Results: The three linear distances, nine angles and two areas differed between the right and left sides of the craniofacial complex ($P < 0.05$) indicate size asymmetry characterized by a wider left side of the face and a shorter vertical dimension on the right side (directional asymmetry). EDMA detected shape asymmetry [T statistic = 2.671 ($P = 0.10$)]. Forty per cent of the EDMA ratios were clinically importantly larger or smaller on the left and right sides respectively, involving landmarks anatomically and morphogenetically important in OFC.

Conclusion: Size and shape directional asymmetries characterize the parental craniofacial skeleton in OFC. This heritable directional craniofacial skeletal asymmetry could be of relevance in the left-sided predilection of OFC.

Index words:

Asymmetry, heritable, morphometric, postero-anterior-cephalogram.

Received 3 October 2001; accepted 13 June 2002

Introduction

Non-syndromic orofacial clefting (OFC) encompasses cleft lip with/or without cleft palate [CL(P)] and isolated cleft palate (CP). Although the overt soft and hard tissue asymmetries are the most obvious craniofacial characteristic in unilateral CL(P), CP can also be an asymmetric defect, where the right or left palatal shelf fuses with the nasal septum. Aetiological heterogeneity (polygenic multifactorial) is currently accepted as being responsible for the majority of cases of OFC, with contributions from genetic and environmental sources.¹ Although a number of cephalometric studies have identified morphological differences between the parents of

children with OFC and comparison groups,² no study has investigated craniofacial asymmetry *per se* as a heritable predisposing factor towards the development of OFC in their offspring. Specifically, the localization and quantification of craniofacial asymmetries could prove to be of crucial significance in the search for the morphogenes involved in OFC.

Asymmetries can be classified as *fluctuating* (FA), *directional* (DA), and *antisymmetry* (AA).³ FA is part of the natural variability, whilst DA can be explained by early embryonic regulation by homeobox genes.⁴ The predilection for left-sided defects in CL(P) is indicative of left-right sided DA. AA is a systematic deviation from symmetry with the larger side varying in the population.

Although the PA cephalogram is arguably the image of choice in the quantification of craniofacial skeletal asymmetries, no basic set of variables is common to several analyses. Most include a variety of linear distance, angular and area parameters to measure size asymmetry. Many analyses compare right- and left-sided measurements to a constructed midline reference plane, despite the curving nature of the biological 'midline' becoming more pronounced with increasingly severe asymmetries. Morphology encompasses size and shape,⁵ however, no PA cephalometric study has analysed *shape* asymmetry. This study investigates skeletal craniofacial asymmetries in the parents of children with OFC using midline landmarks as the mid-facial reference, avoiding the necessity for a constructed reference plane. The size of independent left- and right-sided measurements are compared, whilst Euclidean distance matrix analysis (EDMA)⁶ is used to quantitatively assess shape asymmetry.

Hypotheses

Null: The parents of children with OFC demonstrate craniofacial skeletal symmetry.

Alternate: The parents of children with OFC demonstrate craniofacial skeletal asymmetries.

Materials and methods

This study was a retrospective PA cephalometric asymmetry analysis of the parents of a completely ascertained sample of all children with cleft lip and/or palate born in the West of Scotland between 1980 and 1984. Because this study sought the parents of non-syndromic OFC cases only, from the sample of 286 probands, 90 babies with OFC forming part of a syndrome were excluded. Thus, the parents of 196 babies with non-syndromic OFC were invited to volunteer for a research project, which had ethical approval for obtaining lateral and PA cephalograms. A total of 136 parental pairs replied, however, 32 subjects defaulted for record collection. A careful history was taken to ensure the participants were the biological parents of the cleft proband. Fourteen of the 104 volunteers were excluded because of previous trauma or a poor quality PA cephalogram leaving 92 parental PA cephalograms available for study. Fifty-two volunteers were parents of children with CL(P) and 40 were parents of children with CP. This high CL(P) to

CP ratio is characteristic of the West of Scotland population⁷ compared to a ratio of 2:1 in many other European 'regions'.⁸ The mean age of the parental sample was 37.2 years and was representative of the population when compared to census data.⁹

The PA cephalograms were recorded by one experienced radiographer on a Siemens Orthoceph 10 cephalometer at the Royal Hospital for Sick Children in Glasgow, Scotland. The subjects were positioned with the trans-porionic axis and Frankfort plane horizontal to the floor.¹⁰ Ear-rods and a nasal rest were used to eliminate rotational errors. The source-transporionic axis and transporionic axis-film distances were 152 cm and 12 cm, respectively. The cephalometer settings were 74 Kv, 15 mA with a 0.64-s exposure time for males and 73 Kv, 15 mA, 0.5-s exposure time for females. The magnification factor was standardized at 8 per cent. The PA cephalograms were scanned at 600 DPI and displayed on a PC monitor. The pixel size was 0.051 mm, smaller than the 0.1 mm maximum, as recommended by Quintero *et al.*¹¹ The *x,y* co-ordinates of 29 skeletal landmarks (Table 1) were then digitized from the monitor-displayed image. Twenty-five per cent ($n = 24$) of the images were redigitized 1 month later¹² to evaluate individual landmark intra-operator reproducibility by quantifying random errors and systematic errors using the co-efficient of reliability, and a two-sample *t*-test, respectively. The level of concern was 0.95 for the random error values and $P < 0.1$ for systematic errors. As a result, five landmarks [CG, IO(R), IO(L), Cond(R) and Cond(L)] were excluded, leaving 24 reproducible landmarks for analysis.

Conventional Cephalometric Asymmetry Analysis (CCAA)

Forty variables used in the CCAA (Table 2) were selected to measure right:left *size*-related DA. These were calculated from the coordinate data using a spreadsheet. The linear variables measured the transverse component of the anterior and posterior cranial base, the orbital, maxillary, zygomatic, and nasal regions. The angular measurements represented the right and left zygomata, the maxillary halves and the nasal cavity sides. The areas of the right/left polygons, right/left maxillo-zygomatic complexes, and right/left nasal cavities were calculated. Right:left ratios of the mean values were used to identify the direction of the asymmetry. Two-sample *t*-tests were calculated using the right and left variables.

Table 1 PA cephalogram landmarks

Landmark	Definition
SO(R)	Most superior point on the inner cortical plate of the right orbital rim
GWSO(R)	Intersection of right greater wing of sphenoid and inner cortex of the supero-lateral orbital rim
(R)ZF	Most medial point of the right zygomatico-frontal suture
SO(L)	Most superior point on the inner cortical plate of the left orbital rim
GWSO(L)	Intersection of right greater wing of sphenoid and inner cortex of the supero-lateral orbital rim
MZF(L)	Most medial point of the left zygomatico-frontal suture
MO(R)	Most medial point on the inner cortical plate of the right orbital rim
CG	Most superior point on the crista galli
N	Intersection of the nasal septum and the anterior cranial base—nasion
MO(L)	Most medial point on the inner cortical plate of the left orbital rim
IO(R)	Most inferior point on the inner cortical plate of the right orbital rim
IO(L)	Most inferior point on the inner cortical plate of the left orbital rim
Z(R)	Zygion—most lateral point on the right zygomatic arch
Cond(R)	Condylar—most superior point on the right mandibular condyle
Cor(R)	Most superior point on the right mandibular coronoid process
Mast(R)	Most inferior point on the right mastoid process (apex)
Z(L)	Zygion—most lateral point on the left zygomatic arch
Cond(L)	Condylar—most superior point on the left mandibular condyle
Cor(L)	Most superior point on the left mandibular coronoid process
Mast(L)	Most inferior point on the left mastoid process (apex)
Mx(R)	Maxillare—most medial point on the right maxillary buttress
MX(L)	Maxillare—most medial point on the left maxillary buttress
C(R)	Most lateral point on the inner cortex of the right anterior nasal aperture
IN(R)	Most inferior point on the inner cortex of the right anterior nasal aperture
ANS	Anterior nasal spine—the centre of the intersection of the nasal septum and the palate
IN(L)	Most inferior point on the inner cortex of the left anterior nasal aperture
C(L)	Most lateral point on the inner cortex of the left anterior nasal aperture
Go(R)	Right gonion—the most outward inferior point on the angle of the mandible
Go(L)	Left gonion—the most outward inferior point on the angle of the mandible

Morphometric asymmetry analysis (MAA)

The MAA was used to evaluate *shape*-related asymmetry. Because shape is the information independent of size, location and orientation,⁵ we used the tpsSmall programme (<ftp://life.bio.sunysb.edu/morphmet/tpssmalw32.exe>), which employs Procrustes algorithms to scale the right and left landmark configurations to uniform size, translating them to superimpose the centroids (the geometric mid-point), and iteratively rotating them to minimize the squared differences between landmarks of the configurations. EDMA software⁶ (<http://faith.med.jhmi.edu/>) was then used to analyse shape asymmetry. This program generates a form matrix for the right and left landmark configurations by calculating all the possible Euclidean distances between the landmark pairs. Each corresponding pair of Euclidean distances are systematically compared as a ratio to produce the form-difference matrix (FDM). These are subsequently sorted to rank the elements according to increasing value. The test statistic '*T*' was calculated as the ratio of the largest/smallest elements of the FDM. The null distribution of *T* was calculated using a non-parametric bootstrap technique based on 100 resamples (pseudosamples) and the proportion of bootstrapped *T*'s greater than *T* are represented as a *P*-value.

Results

The results from the CCAA are shown in Tables 3–5. Three linear distance measurements were highly statistically significantly different on the right and left sides ($P < 0.01$). All were larger on the left: facial width (measured to ANS), maxillary width and nasal width. All the angles in the maxilla and zygoma statistically significantly differed on the right and left ($P < 0.05$), but no one side dominated by having the larger mean measurement. The polygon area was statistically significantly larger on the right ($P = 0.003$), whereas, the nasal area was statistically significantly larger on the left side ($P = 0.002$).

The EDMA *T* statistic was 2.671, demonstrating significant morphological variation between the right and left sides of the craniofacial complex ($P = 0.010$; Table 6). The median ratio was 1.000: between SO-IN. There were no ratios between 1.4–1.5. The 47 ratios in the groups 0.9–1.0 and 1.0–1.1 (60 per cent of the total ratios) involve less than a 10 per cent difference in morphology between the right and left sides. These are

Table 2 Variables selected for conventional metric asymmetry analysis

	Region described	Right	Left
Linear distances	Anterior cranial base	GWSO(R)-N	N-GWSO(L)
	Inner orbital width	MO(R)-N	N-MO(L)
	Facial width	Z(R)-N	N-Z(L)
	Facial width	Z(R)-ANS	ANS-Z(L)
	Mastoid width	MAST(R)-ANS	ANS-MAST(L)
	Maxillary width	MX(R)-ANS	ANS-MX(L)
	Nasal width	C(R)-ANS	ANS-C(L)
	Width of nasal floor	IN(R)-ANS	ANS-IN(L)
Angles	Maxillozygomatic complex	ANS-MZF(R)-Z(R)	ANS-MZF(L)-Z(L)
	Maxillozygomatic complex	ANS-Z(R)-MZF(R)	ANS-Z(L)-MZF(L)
	Maxillozygomatic complex	MZF(R)-ANS-Z(R)	MZF(L)-ANS-Z(L)
	Maxillozygomatic complex	ANS-Z(R)-MX(R)	ANS-Z(L)-MX(L)
	Maxillozygomatic complex	ANS-MX(R)-Z(R)	ANS-MX(L)-Z(L)
	Maxillozygomatic complex	Z(R)-ANS-MX(R)	Z(L)-ANS-MX(L)
	Nasal cavity	N-C(R)-ANS	N-C(L)-ANS
	Nasal cavity	N-ANS-C(R)	N-ANS-C(L)
Areas	Nasal cavity	C(R)-N-ANS	C(L)-N-ANS
	Right/left polygon	SO(R)-N-ANS + SO(R)-GWSO(R)-ANS + GWSO(R)-MZF(R)-ANS + MZF(R)-Z(R)-ANS + Z(R)-MX(R)-ANS	SO(L)-N-ANS + SO(L)-GWSO(L)-ANS + GWSO(L)-MZF(L)-ANS + MZF(L)-Z(L)-ANS + Z(L)-MX(L)-ANS
	Right/left maxilla + zygoma	ANS-MZF(R)-Z(R) + ANS-Z(R)-MX(R) MX(L)	ANS-MZF(L)-Z(L) + ANS-Z(L)-
	Right/left nasal cavity	N-C(R)-ANS	N-C(L)-ANS

Table 3 Linear distance measurements: means, SD, right/left ratios, and two-sample *t*-test results

Variable	Right (mm)	Left (mm)	Ratio (R:L)	<i>P</i> -value (R:L)
GSWO-N	57.2 (2.4)	57.1 (2.6)	1.001	0.922
MO-N	16.4 (2.0)	15.9 (2.1)	1.028	0.348
Z-N	87.4 (4.3)	88.0 (4.9)	0.994	0.053
Z-ANS	88.5 (5.3)	89.5 (5.7)	0.99	0.007**
Mast-ANS	70.5 (4.6)	72.2 (4.3)	0.977	0.317
Mx-ANS	36.6 (2.5)	37.7 (2.6)	0.973	0***
C-ANS	21.4 (2.3)	21.7 (2.7)	0.99	0.006**
IN-ANS	11.0 (1.9)	11.3 (2.0)	0.937	0.211

p*<0.05; *p*<0.01; ****p*<0.001.

not clinically important as minor right/left asymmetries are part of normal variation. Table 6 and Figure 1 display the clinically important ratios, with the smaller ratios depicted on the right side of the craniofacial complex and the larger ratios on the left. The ratios 0.6–0.7, 0.7–0.8, and 0.8–0.9 all involve the landmarks N and ANS. Ratios 1.1–1.2, 1.2–1.3, 1.3–1.4, 1.5–1.6, and 1.6–1.7 all involved the landmarks C and MO, the only exception being the ratio GWSO-MZF (1.150).

Discussion

The results from the CCAA and the MAA do not support the null hypothesis—that of skeletal symmetry. Instead, the results support the alternate hypothesis—that skeletal asymmetry is present in the parental craniofacial complex in OFC and by virtue of the heritability of craniofacial morphology, influences the development of OFC in their offspring.

Table 4 Angular measurements: means, SD, right/left ratios and two-sample *t*-test results

Variable	Right (°)	Left (°)	Ratio	<i>P</i> -value
Maxilla + zygoma				
ANS-MZF-Z	83.5(9.6)	83.8(9.7)	0.086	0***
ANS-Z-MZF	71.5(7.1)	70.5(7.1)	1.02	0***
MZF-ANS-Z	24.8(4.3)	25.5(4.2)	0.975	0***
ANS-Z-MX	18.6(2.9)	18.9(2.9)	0.99	0***
ANS-MX-Z	128.8(9)	129.2(8.4)	0.998	0***
Z-ANS-MX	32.4(6.6)	31.8(6.2)	1.032	0***
Nasal cavity				
N-C-ANS	96.8(6.6)	95.6(6.8)	1.015	0***
N-ANS-C	62.2(5.5)	63.1(5.7)	0.989	0***
C-N-ANS	20.9(2.7)	21.1(2.8)	0.993	0.024*

p*<0.05; *p*<0.01; ****p*<0.001.

Table 5 Area measurements: means, SD, right/left ratios and two-sample *t*-test results

Variable	Right (mm ²)	Left (mm ²)	Ratio	<i>P</i> -value
Polygon area	5777 (560)	4602 (426)	1.177	0.003**
Maxilla + zygoma area	2469 (215)	2493 (297)	0.967	0.529
Nasal cavity area	577 (32)	589 (39)	0.988	0.002**

p*<0.05; *p*<0.01; ****p*<0.001.

The statistically significant linear distance measurements were all of greater magnitude on the left side of the face—indicative of DA. Interestingly, all the angles differed on the right and left sides, demonstrating a morphological difference between the right and left sides of the maxillo-zygomatic complex. Despite the larger right hemifacial area conflicting with the directional nature of the linear measurements, the nasal cavity area was larger on the left. These features indicate a general tendency to a wider left side of the face and a shorter vertical dimension on the right side of the face in the parents of children with OFC.

EDMA detected a statistically significant shape asymmetry, involving a range of morphological differences between the right and left sides of the craniofacial complex, as demonstrated by the *T* statistic (2.671). The clinically important ratios less than 1.000 all involved the landmarks N and ANS, whereas those greater than 1.000 almost exclusively involved the landmarks C and MO. Furthermore, these clinically important larger and smaller ratios exclusively involved the left and right sides respectively. Thus, in addition to directional size asymmetry, the parental craniofacial complex in OFC is characterized by a directional shape asymmetry. Could our finding of directional asymmetry in the parental

craniofacial complex in OFC be related to the predilection to left sided clefts? Furthermore, the influential landmarks that were detected using EDMA were ANS, N, C and MO. These are all anatomically and morphogenetically closely related to the oro-nasal region and the morphogenes that code for this region are likely to be of crucial significance in the aetiopathogenesis of OFC.

Morphology comprises size and shape,⁵ and although ideal, there are no cephalometric tools that can rigorously evaluate size *and* shape simultaneously. Therefore, our strategy synthesizing the information obtained from a conventional cephalometric asymmetry analysis and a morphometric asymmetry analysis is valid. In particular, the search for OFC morphogenes will be assisted considerably by the availability of shape-asymmetry information. It seems surprising therefore, that no cephalometric study has specifically evaluated shape asymmetry, a defining phenotypic characteristic of the craniofacial complex in OFC.

Nevertheless, there are limitations associated with this study. Controls were not available to determine the level of asymmetry in the Scottish population. It is assumed that, although FA is present in the population, overall AA will result where the population level of craniofacial asymmetry is zero. Furthermore, retrospective studies

Table 6 Ten per cent extremities of the sorted form-difference matrix

Euclidean distance	Ratio
COR-ANS	0.608
MX-ANS	0.630
SO-N	0.643
GWSO-N	0.670
MZF-N	0.689
MAST-ANS	0.700
Z-ANS	0.715
MZF-ANS	0.766
GWSO-ANS	0.792
N-Z	0.809
N-COR	0.833
SO-ANS	0.834
N-ANS	0.869
N-MAST	0.880
MO-ANS	0.891
SO-IN	1.000
MO-MAST	1.113
N-C	1.133
GWSO-MZF	1.150
MO-C	1.162
SO-C	1.197
MO-Z	1.230
MO-COR	1.256
GWSO-C	1.277
MZF-C	1.309
MAST-C	1.364
Z-C	1.382
GWSO-MO	1.500
SO-MO	1.506
MZF-MO	1.507
MX-C	1.540
COR-C	1.625

Median ratio in bold.

T statistic (max/min): 2.671; *P* = 0.010.

are associated with inherent biases, which we attempted to minimize. Our experimental group were identified from a completely ascertained sample of children with non-syndromic OFC from a record registry. This reduced the principal bias in a case-control study: subjectivity in the selection of the parental sample. Volunteer bias is unavoidable in a study involving ionizing radiation, although there is no reason to suspect that the opinions of individual volunteers about ionizing radiation would introduce biologically significant variation in the craniofacial morphology of case parents. Furthermore, in spite of the parental sample not being a consecutive sample, including *both* biological parents of *each successive* cleft child-birth, the ratio of CL(P) to CP in the children of the parental group was similar to that of published data

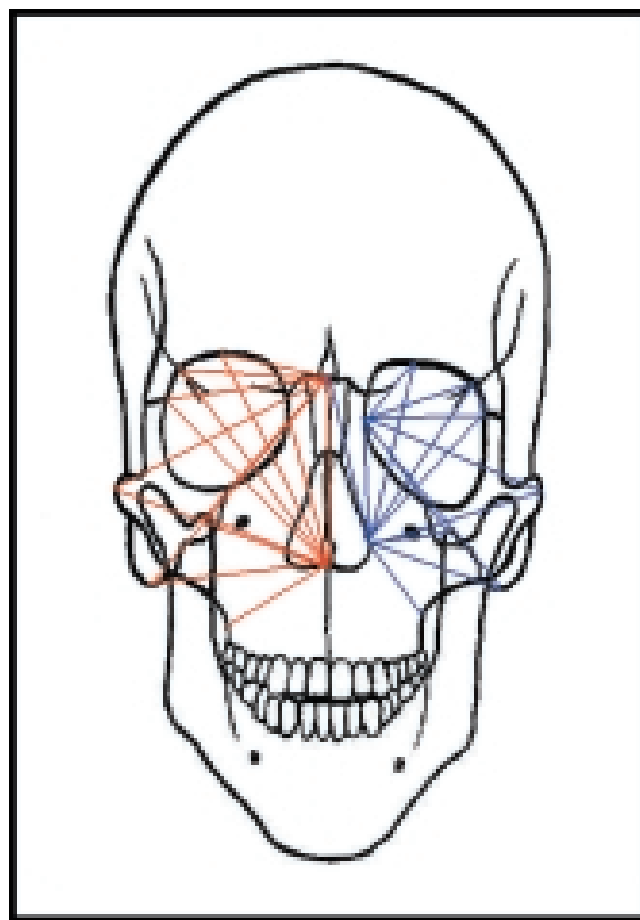


Fig. 1 Clinically important ratios of Euclidean distances. Red lines = smaller Euclidean distances. Blue lines = larger Euclidean distances.

for the Scottish population.⁷ Thus, the parental group accurately represented the parents of children with OFC resident in the West of Scotland.

Further work required

Consistency of association of information derived from the parental craniofacial phenotype in investigations in disparate ethnic groupings and worldwide regions would potentially inform the ongoing investigation of the candidate genes involved in OFC. Further studies evaluating size- and shape-related asymmetry in unoperated and operated individuals with OFC, their non-cleft parents and siblings in different population groups are required.

Conclusions

Size and shape directional asymmetries characterize the parental craniofacial complex in OFC. This heritable

directional craniofacial skeletal asymmetry could be of considerable relevance in the left-sided predilection of OFC.

Acknowledgements

This study is supported by a European Orthodontic Society W. J. B. Houston Research Grant.

References

1. Mossey PA, McColl J, O'Hara M. Cephalometric features in the parents of children with orofacial clefting. *Br J Oral Maxillofac Surg* 1998; **36**: 202–12.
2. McIntyre GT, Mossey PA. The craniofacial morphology of the parents of children with orofacial clefting: a systematic review of cephalometric studies. *J Orthod* 2002; **29**: 23–9.
3. Auffray J-C, Debat V, Alibert P. Shape asymmetry and developmental stability. In Chaplain MA, Singh GD, McLachlan JC, eds, *On Growth and Form Spatio-temporal Pattern Formation in Biology*. Chichester: Wiley, 1999, pp. 309–24.
4. Pirttiniemi P. Normal and increased functional asymmetries in the craniofacial area. *Acta Odontol Scand* 1998; **56**: 342–5.
5. McIntyre GT, Mossey PA. Size and shape measurement in contemporary cephalometrics. *Eur J Orthod*. [In press].
6. Cole TM. *WinEDMA: software for Euclidean Distance Matrix Analysis*. Kansas City: University of Missouri – Kansas City School of Medicine, 1999.
7. Fitzpatrick DR, Raine PA, Boorman JG. Facial clefts in the West of Scotland 1980–84: epidemiology and genetic diagnoses. *J Med Genet* 1994; **31**: 126–9.
8. Jensen BL, Kreiborg S, Dahl E, Fogh-Andersen P. Cleft lip and palate in Denmark 1976–1981. Epidemiology, variability and early somatic development. *Cleft Palate J* 1988; **25**: 258–69.
9. *The 1981 census on CD-Rom*. Oxford: Chadwyck-Healey, 1991.
10. Grummons DC, Kappeyne MA. A frontal asymmetry analysis. *J Clin Orthod* 1987; **21**: 448–65.
11. Quintero JC, Trosien A, Hatcher D, Kapila S. Craniofacial imaging in orthodontics: historical perspective, current status, and future developments. *Angle Orthod* 1999; **69**: 491–506.
12. Houston WJ. The analysis of errors in orthodontic measurements. *Am J Orthod Dentofac Orthop* 1983; **83**: 382–90.

